

Flóra Hajdú,<sup>1</sup>  Péter Mika,<sup>2</sup>  Péter Szalai,<sup>3</sup>  Rajmund Kuti<sup>4</sup> 

# Road Profile Modelling Based on Measurement for Fire Truck Simulation

*The unevenness of the road reduces the life of the vehicle's suspensions, and the resulting harmful vibrations can also lead to the failure of other structures. In case of special superstructures like fire trucks, valuable firefighting equipment can also be damaged. Since there is little available literature dealing with the vibrations generated during the use of firefighting vehicles, in this research work a real road profile based on data from geodetic measurements was generated for numerical simulation. The suspension of the vehicle taking into account the parameters of a heavy-duty firefighting vehicle was also modelled, and then the effects of road failures using computer simulation were investigated. The road profile was implemented in the simulations with spline polynomials and the fire truck was simulated as a full vehicle model. The aim of the research is to compare the achieved simulation results with data from other vehicle research studies, thereby achieving more accurate results that can also be applied in practice, contributing to vehicle design and safe operation.*

**Keywords:** road profile generation, road profile measurement, fire truck, numerical simulation, vibration

## Introduction

An important aspect of the vibration simulation of vehicle suspensions is the modelling of the road as an excitation signal. Vibrations caused by road failures can damage the vehicle and

---

<sup>1</sup> Assistant Professor, Széchenyi István University, Faculty of Mechanical Engineering, Informatics and Electrical Engineering, Department of Machine Design, e-mail: [hajdf@sze.hu](mailto:hajdf@sze.hu)

<sup>2</sup> Assistant Lecturer, Széchenyi István University, Faculty of Mechanical Engineering, Informatics and Electrical Engineering, Department of Machine Design, e-mail: [mika.peter@sze.hu](mailto:mika.peter@sze.hu)

<sup>3</sup> Master Lecturer, Széchenyi István University, Faculty of Mechanical Engineering, Informatics and Electrical Engineering, Department of Machine Design, e-mail: [szalai@sze.hu](mailto:szalai@sze.hu)

<sup>4</sup> Full Professor, Széchenyi István University, Faculty of Mechanical Engineering, Informatics and Electrical Engineering, Department of Automation and Mechatronics, e-mail: [kuti.rajmund@sze.hu](mailto:kuti.rajmund@sze.hu)

the passengers and have safety-related issues.<sup>5</sup> They impair the controllability of vehicles,<sup>6</sup> reduce travel comfort<sup>7</sup> and can be the main causes of fatigue of individual components,<sup>8</sup> and can even cause immediate suspension failure or component breakage.<sup>9</sup> The road profile has effects on fuel consumption, tire wear, maintenance cost and vehicle delay costs.<sup>10</sup> Most of the harmful vibrations in vehicles occur while driving, and the road itself is the triggering factor.

The examination of various vibrations on vehicles was mostly carried out in case of passenger cars,<sup>11</sup> or different trucks,<sup>12</sup> and there are only some examples of fire trucks.<sup>13</sup> Therefore, a heavy-duty firefighting vehicle was chosen in our study, because its structural elements differ from other vehicles, and harmful vibrations can damage valuable firefighting equipment. The goal is to achieve results that can be used as a basis point for further research and field measurements.

This paper presents the numerical examination of a heavy-duty fire truck with a random excitation signal based on road profile measurements. First, a short theoretical overview of random road profiles is presented which is followed by road profile measurements. Then, the fire truck model is discussed followed by the simulation results. The simulation results were compared to the literature and field measurements.

## Road profile modelling

In case of vehicle simulations, mostly theoretical or standardised road profiles are used.<sup>14</sup> The basis of road profile modelling is the ISO 8068 standard.<sup>15</sup> The standard takes the power spectral density (PSD) of the road profile into account. The road profile is calculated with the following equations.<sup>16</sup>

$$\Phi(\Omega) = \Phi(\Omega_0) \left( \frac{\Omega}{\Omega_0} \right)^{-w} \quad (1)$$

$$\Phi(n) = \Phi(n_0) \left( \frac{n}{n_0} \right)^{-w} \quad (2)$$

where

$$\bullet \quad \Omega = \frac{2\pi}{L} \left[ \frac{rad}{m} \right] \text{ angular spatial frequency}$$

<sup>5</sup> GEBRESENBET et al. 2011: 10–19.

<sup>6</sup> GILLESPIE–SAYERS 1981.

<sup>7</sup> LAKUŠIĆ et al. 2011: 485–494.

<sup>8</sup> BOGSJÖ–RYCHLIK 2009: 391–402.

<sup>9</sup> MATSIKA 2001.

<sup>10</sup> YOUSEFZADEH et al. 2010: 743–754.

<sup>11</sup> BURDZIK–KONIECZNY 2014: 83–90; LITAK et al. 2008: 1373–1383.

<sup>12</sup> FAHAD et al. 2022: 66–71; ŞENDUR et al. 2013; ZHAO et al. 2016: 1–9.

<sup>13</sup> KOVTUN et al. 2018; KOVTUN et al. 2019: 495–500.

<sup>14</sup> MÚČKA 2018; ZEIDI et al. 2017: 285–295.

<sup>15</sup> ISO 8608:2016.

<sup>16</sup> TYAN et al. 2009: 151–156.

- $L$  wavelength
- $\Phi_0 = \Phi(\Omega_0) \left[ \frac{m^2}{rad/m} \right]$  values of the PSD at reference wave number  $\Omega_0 = 1 \frac{rad}{m}$
- $n = \frac{\Omega}{2\pi}$  spatial frequency,  $n_0 = 0.1 \frac{cycle}{m}$
- $w$  waviness, for most of the road surface  $w = 2$

There are several approaches to generate random road profiles based on the standard, which are white noise filtration, moving average of white noise, sinusoidal approximation, Gaussian white noise, hybrid approach, Laplace processes and Gaussian random field.<sup>17</sup>

Lenkútis et al. (2021) compares the white noise filtration, the sinusoidal approach and the moving average of white noise. In case of the white noise filtration, a white noise signal is transformed into a road profile through a first-order linear shape filter. This method is easy to implement but sensitive to the adjustable parameters and the vehicle speed. In case of the sinusoidal method, the road profile can be generated from a set of sinusoidal waves with different phases, amplitudes and wavelengths. The advantages of the method are that more parameters can be controlled, and numerical errors are avoided by obtaining the road profile height without going through the numerical differentiation. It is the most time-consuming method and duplicates profile fragments. "The moving average of white noise is a convolution of a kernel function with an infinitesimal white noise process having the variance equal to the spatial discretization step."<sup>18</sup> This method and the white noise filtration do not duplicate profile fragments. Tyan et al. (2009) compares the shaping filter and the sinusoidal approximation. In case of the shaping filter, it was found that the time constant of the transfer function is independent of the road profile grade. In case of the sinusoidal approach, it was obtained that the amplitude of each sinusoidal function is proportional to the square root of the related PSD. In the paper of Dharankar et al. (2017), random road profiles are generated using white noise filtration and superposition of harmonics (sinusoidal method). The statistical analysis of the generated road profiles is also presented to evaluate the efficacy of the presented methods. It was observed that white noise filtration with a low-frequency cut-off is suitable for random road profile generation but only for particular types of roads. It also has a large difference compared to the ISO standard in case of low frequencies. The sinusoidal approximation is a flexible and powerful technique to generate a random road profile from its spectral description. It provides the generation of the signal with its differentiations without going through numerical differentiation and therefore numerical errors can be avoided. In the paper of Agostinacchio et al. (2014), the sinusoidal approach was used to generate random road profiles. The force exchange between the pavement and different types of vehicles was examined using Matlab. It was shown that the vibrational stress from the vehicle can be

<sup>17</sup> LENKUTIS et al. 2021.

<sup>18</sup> LENKUTIS et al. 2021.

determined as a function of the pavement's surface degradation, and the speed and type of the vehicle. The quarter car model was used for the simulation.

In this study, the sinusoidal approach was selected, because of the ability to avoid numerical errors and it is based on the PSD of the road. In this case, the random road profile can be generated with the following formula:<sup>19</sup>

$$h(y) = \sum_{i=0}^N \sqrt{\Delta n} 2^k 10^{-3} \left( \frac{n_0}{i \Delta n} \right) \cos(2\pi i \Delta n y + \varphi_i) \quad (3)$$

where  $h(y)$  is the amplitude of the road profile,  $y$  is the displacement,  $\varphi_i$  is a random phase angle, and  $k$  is a coefficient based on the road class (see Table 1).

Table 1: Road profile classification

Road class		k
A	B	3
B	C	4
C	D	5
D	E	6
E	F	7
F	G	8
G	H	9

Source: Compiled by the authors based on AGOSTINACCHIO et al. 2014: 270.

## Road profile measurement

There are several road profile measurement methods. "Most of them measure vertical deviations of the road surface along the traveling wheel path."<sup>20</sup> The types of road profile measuring equipment can be divided into the following groups: response-type road roughness measuring systems, high-speed inertial profilers, profilographs, lightweight profilers, manual devices and longitudinal profile analysers. Nowadays, road profile estimation from the measured acceleration of the vehicle is spreading. To reduce the inaccuracies from the measuring device and the vehicle, artificial neural networks are developed to determine the road profile.<sup>21</sup> In the paper of Zhao et al. (2019), a road profile estimation method using a smartphone is presented. First, the parameters of the vehicle are identified using a known-size hump. Then the road profile is estimated based on acceleration data measured by the smartphone using an augmented Kalman filter. The estimated profiles are compared with a profile measured by a laser profiler. In the paper of Lee et al. (2017), the development of a 3D profilometer to measure unpaved roads is presented. A virtual road model was also

<sup>19</sup> AGOSTINACCHIO et al. 2014: 267–275.

<sup>20</sup> YOUSEFZADE et al. 2010: 743–754.

<sup>21</sup> YOUSEFZADE et al. 2010: 743–754.

created, which was used in vehicle simulation. In the paper of Eshkabilov and Yunusov (2018), the road profile is measured using accelerometers installed on the front axle and the body of a car and a roughometer. For reference, the road profile was measured with a geometry-based approach too. A 100 m long asphalt pavement road was measured with a sampling frequency of 0.25 m per 1 m. In the paper of Li et al. (2015), a method of measuring asphalt pavement texture depth based on structured-light technology is proposed. The 3D data for the asphalt pavement was collected by laser triangulation using infrared lasers and an area-array camera. The asphalt pavement texture depth was calculated based on the 3D data.

For road profile measurement the geometric-based approach was selected as it was used to validate the measurement according to the literature.<sup>22</sup> The road profile was measured using a Leica Disto S910 Laser Distance Meter digital laser meter. The points were measured in the width of the wheel of the fire truck. The height of the points was measured relative to a starting point. The device measures the vertical inclination, determines the direct distance between the gauge and the object, and calculates the vertical distance from the horizontal baseline by trigonometric calculation (Figure 1).

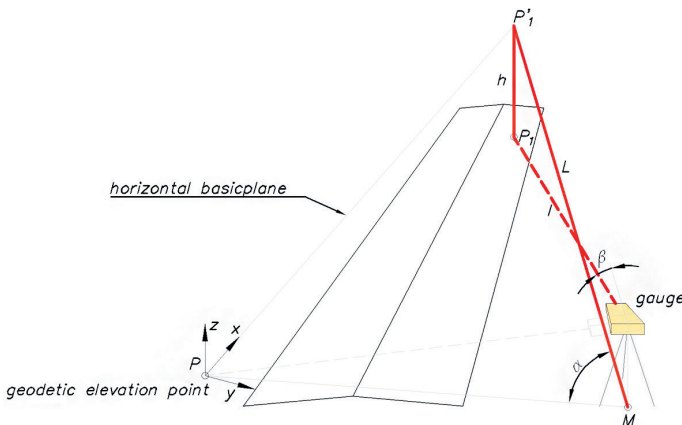


Figure 1: Measurement principle (right)

Source: Compiled by the authors.

The points M–P– $P_1$  stretch the horizontal base plane, which lies on a measured geodetic point. The instrument places the coordinate system on the first measured point. The x direction adjusts to the direction of the second point, while measuring the angle of horizontal rotation ( $\alpha$ ) and vertical rotation ( $\beta$ ). Knowing the vertical angle, the legs of right-angled triangles can be calculated using the angle function, thus obtaining the horizontal distance (L) and the height difference (h).

Several technical parameters can be used to determine the longitudinal surface unevenness of the road surface.

- International Inequality Index (IRI)

<sup>22</sup> ESHKABILOV–YUNUSOV 2018: 24–40.

- roughness
- wavelength
- longitudinal profile variance
- spectral density
- standard deviation

The most common technical parameter is IRI. When determining the wavelength, a 100 m section was chosen in Germany. In Belgium and the Czech Republic, it is determined using non-contact technology and a measurement length of 100 m. In the United Kingdom, the variance of the longitudinal profile is determined by sampling every 10 m.

So, taking the above into account, it can be said that in the case of longitudinal undulations, 10 m sampling is sufficient. We chose 0.25 m, which is already sufficient for vibration simulation.

The smallest measurable irregularity depends on the measuring instrument. Micro, macro and mega roughness are distinguished in the literature.<sup>23</sup> The micro roughness refers to wavelengths smaller than 0.5 mm. The macro roughness is between 0.5 mm and 50 mm. Finally, the mega roughness means a wavelength over 50 mm.

But taking into account the grain size in the pavement surface, a difference of less than 1 cm is not worth showing.

The measured road profile was selected in Nép street in Győr. The selected section is a sixth category road<sup>24</sup> with a traffic of 1,500–3,000 vehicles per day and very bad pavement condition. A 100 m section was selected for measurement and simulations. The measured road profiles are shown in Figure 2.

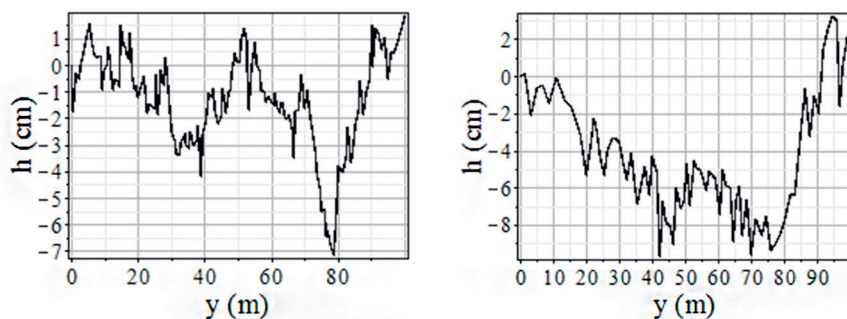


Figure 2: Measured road profiles  
Source: Compiled by the authors.

The spatial frequency was large (70 cm), therefore instead of calculating the PSD, a statistical analysis was carried out to obtain the class of the road. Different road profiles were generated and then they were compared with the measured road profile. The minimum, maximum and

<sup>23</sup> COST 2007: 354; GÁSPÁR–KÁROLY 2007: 442–449.

<sup>24</sup> GÁSPÁR et al. 2011.

average values and the deviation were calculated. The measured average value in the case of the measured road profile should be first corrivated to compare with the generated road profile. The statistical analysis is shown in Table 2. Based on the statistical analysis it is an ISO C–D profile, which is a low-quality paved road.<sup>25</sup>

Table 2: Statistical analysis of the road profiles

	k = 4	k = 5	k = 6	Left	Left corr.	Right	Right corr.
minimum (m)	-0.0366	-0.0605	-0.1054	-0.0715	-0.0585	-0.0970	-0.0516
maximum (m)	0.0258	0.0598	0.1555	0.0186	0.0316	0.0324	0.0778
average (m)	0	0	0	-0.0130		-0.0454	
deviation (m)	0.01450	0.0290	0.0580	0.0180		0.0323	

Source: Compiled by the authors.

### Vehicle simulation

The vehicle model was based on a Csepel D755-10 fire heavy-duty fire truck.<sup>26</sup> As the aim of the study was road profile modelling and to test it in a simulation environment, therefore, the fire truck was modelled as a linear full vehicle model to generate 2 different road profiles to the left and right sides. The model can be seen in Figure 3.

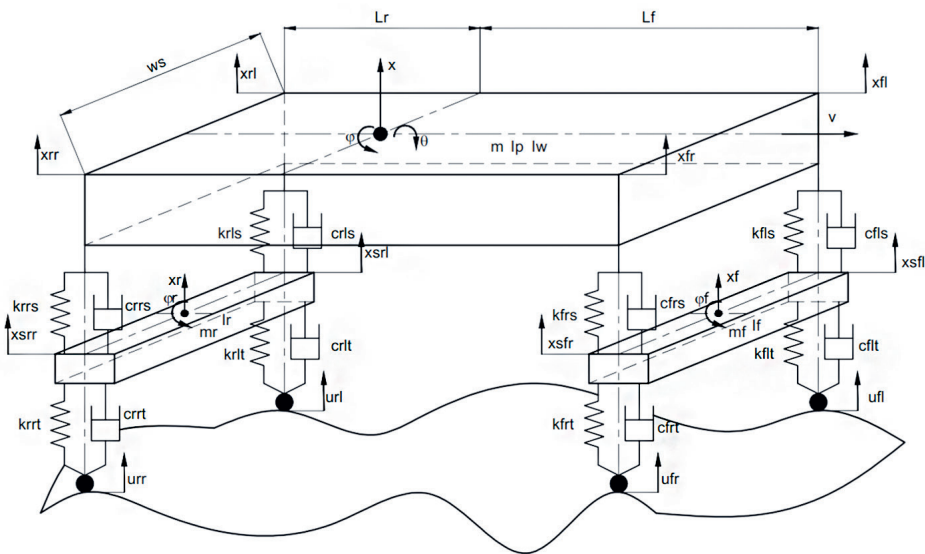


Figure 3: Full car model of the heavy-duty fire truck

Source: Compiled by the authors.

<sup>25</sup> MÚČKA 2018.

<sup>26</sup> HAJDU et al. 2019: 51–62.

The differential equations describing the system's behaviour can be obtained with free-body diagrams.<sup>27</sup>

$$m\ddot{x} + k_{rrs}(x_{rr} - x_{srr}) + k_{rls}(x_{rl} - x_{srl}) + k_{frs}(x_{fr} - x_{sfr}) + k_{fls}(x_{fl} - x_{sfl}) + c_{rrs}(\dot{x}_{rr} - \dot{x}_{srr}) + c_{rls}(\dot{x}_{rl} - \dot{x}_{srl}) + c_{frs}(\dot{x}_{fr} - \dot{x}_{sfr}) + c_{fls}(\dot{x}_{fl} - \dot{x}_{sfl}) = 0 \quad (4)$$

$$I_p\ddot{\theta} + L_r k_{rrs}(x_{rr} - x_{srr}) + L_r k_{rls}(x_{rl} - x_{srl}) - L_f k_{frs}(x_{fr} - x_{sfr}) - L_f k_{fls}(x_{fl} - x_{sfl}) + L_r c_{rrs}(\dot{x}_{rr} - \dot{x}_{srr}) + L_r c_{rls}(\dot{x}_{rl} - \dot{x}_{srl}) - L_f c_{frs}(\dot{x}_{fr} - \dot{x}_{sfr}) - L_f c_{fls}(\dot{x}_{fl} - \dot{x}_{sfl}) = 0 \quad (5)$$

$$I_w\ddot{\varphi} + \frac{W_s}{2} k_{rrs}(x_{rr} - x_{srr}) + \frac{W_s}{2} k_{rls}(x_{rl} - x_{srl}) - \frac{W_s}{2} k_{frs}(x_{fr} - x_{sfr}) - \frac{W_s}{2} k_{fls}(x_{fl} - x_{sfl}) + \frac{W_s}{2} c_{rrs}(\dot{x}_{rr} - \dot{x}_{srr}) + \frac{W_s}{2} c_{rls}(\dot{x}_{rl} - \dot{x}_{srl}) - \frac{W_s}{2} c_{frs}(\dot{x}_{fr} - \dot{x}_{sfr}) - \frac{W_s}{2} c_{fls}(\dot{x}_{fl} - \dot{x}_{sfl}) = 0 \quad (6)$$

$$m_r\ddot{x}_r + k_{rrs}(x_{srr} - x_{rr}) + k_{rls}(x_{srl} - x_{rl}) + k_{rrt}(x_{srr} - u_{rr}) + k_{rlt}(x_{srl} - u_{rl}) + c_{rrs}(\dot{x}_{srr} - \dot{x}_{rr}) + c_{rls}(\dot{x}_{srl} - \dot{x}_{rl}) + c_{rrt}(\dot{x}_{srr} - \dot{u}_{rr}) + c_{rlt}(\dot{x}_{srl} - \dot{u}_{rl}) = 0 \quad (7)$$

$$I_r\ddot{\varphi}_r + \frac{W_s}{2} k_{rrs}(x_{srr} - x_{rr}) + \frac{W_s}{2} k_{rls}(x_{srl} - x_{rl}) + \frac{W_s}{2} k_{rrt}(x_{srr} - u_{rr}) + \frac{W_s}{2} k_{rlt}(x_{srl} - u_{rl}) + \frac{W_s}{2} c_{rrs}(\dot{x}_{srr} - \dot{x}_{rr}) + \frac{W_s}{2} c_{rls}(\dot{x}_{srl} - \dot{x}_{rl}) + \frac{W_s}{2} c_{rrt}(\dot{x}_{srr} - \dot{u}_{rr}) + \frac{W_s}{2} c_{rlt}(\dot{x}_{srl} - \dot{u}_{rl}) = 0 \quad (8)$$

$$m_f\ddot{x}_f + k_{frs}(x_{sfr} - x_{fr}) + k_{fls}(x_{sfl} - x_{fl}) + k_{frt}(x_{sfr} - u_{fr}) + k_{flt}(x_{sfl} - u_{fl}) + c_{frs}(\dot{x}_{sfr} - \dot{x}_{fr}) + c_{fls}(\dot{x}_{sfl} - \dot{x}_{fl}) + c_{frt}(\dot{x}_{sfr} - \dot{u}_{fr}) + c_{flt}(\dot{x}_{sfl} - \dot{u}_{fl}) = 0 \quad (9)$$

$$I_f\ddot{\varphi}_f + \frac{W_s}{2} k_{frs}(x_{sfr} - x_{fr}) + \frac{W_s}{2} k_{fls}(x_{sfl} - x_{fl}) + \frac{W_s}{2} k_{frt}(x_{sfr} - u_{fr}) + \frac{W_s}{2} k_{flt}(x_{sfl} - u_{fl}) + \frac{W_s}{2} c_{frs}(\dot{x}_{sfr} - \dot{x}_{fr}) + \frac{W_s}{2} c_{fls}(\dot{x}_{sfl} - \dot{x}_{fl}) + \frac{W_s}{2} c_{frt}(\dot{x}_{sfr} - \dot{u}_{fr}) + \frac{W_s}{2} c_{flt}(\dot{x}_{sfl} - \dot{u}_{fl}) = 0 \quad (10)$$

where

$$x_{rr} = x + L_r\theta - \frac{W_s}{2}\varphi \quad (11)$$

$$x_{rl} = x + L_r\theta + \frac{W_s}{2}\varphi \quad (12)$$

$$x_{fr} = x - L_f\theta - \frac{W_s}{2}\varphi \quad (13)$$

<sup>27</sup> HORVÁTH 2006.

$$x_{fl} = x - L_f \theta + \frac{w_s}{2} \varphi \quad (14)$$

$$x_{srr} = x_r - \frac{w_s}{2} \varphi_r \quad (15)$$

$$x_{srl} = x_r + \frac{w_s}{2} \varphi_r \quad (16)$$

$$x_{sfr} = x_l - \frac{w_s}{2} \varphi_l \quad (17)$$

$$x_{sfl} = x_l + \frac{w_s}{2} \varphi_l \quad (18)$$

The mass parameters were taken from the manufacturer's catalogue. The moment of inertia of the axles was calculated with CAD software. The parameters of spring stiffness and the damping coefficients were taken from the literature.<sup>28</sup> The parameters used for the simulation are listed in Table 3.

Table 3: Simulation parameters

Parameter	Value	Unit
$m$	14,400	kg
$m_r$	1,480	kg
$m_f$	620	kg
$I_p$	58,000	kgm <sup>2</sup>
$I_w$	17,500	kgm <sup>2</sup>
$I_r$	250	kgm <sup>2</sup>
$I_f$	160	kgm <sup>2</sup>
$w_s$	2.2	m
$L_r$	0.613	m
$L_f$	3.486	m
$k_{rrs}, k_{rls}$	400,000	N/m
$k_{frs}, k_{fls}$	0.613	N/m
$c_{rrs}, c_{rls}$	3.486	Ns/m
$c_{frs}, c_{fls}$	20,000	Ns/m
$k_{rrt}, k_{rlt}$	1,800,000	N/m
$k_{frt}, k_{flt}$	1,000,000	N/m
$c_{rrt}, c_{rlt}$	1,000	Ns/m
$c_{frt}, c_{flt}$	500	Ns/m

Source: Compiled by the authors.

<sup>28</sup> JIAO 2013.

For numerical simulations, Maple 17 was used. Rkf45 numerical algorithm was used with step size 0.01 s. A C–D class road with  $k = 5$  was generated. The frequency band was divided into 1,000 intervals. A 100 m long road profile was generated. The horizontal distance of the road profile was converted into time as a function of speed, then the excitation signals on the tires were calculated as third-degree spline polynomials, which were used as mathematical equations in the simulation ( $u_{rr}(t), u_{rl}(t), u_{fr}(t), u_{fl}(t)$ ). A time delay was included between the front and rear suspension:

$$T_d = \frac{Lr + Lf}{v} \tag{19}$$

where  $v$  is the vehicle's speed. This time delay is 0.3 s if the vehicle speed is 50 km/h.

The vehicle speed was 50 km/h. The displacement of the body and the axles is shown in Figure 4.

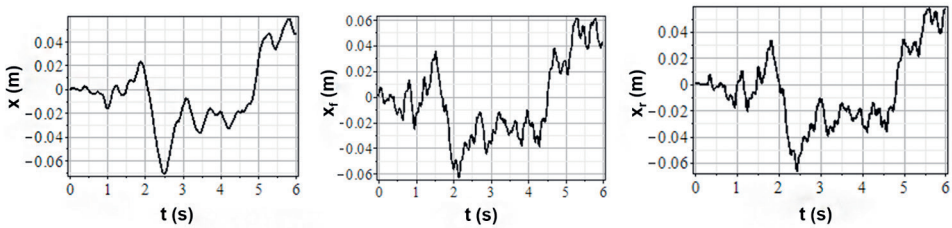


Figure 4: Displacement of the body (left), front axle (middle) and rear axle (right)  
 Source: Compiled by the authors.

The maximum displacement is 0.06 m. A time delay between the front and rear axle can be observed. Besides the time delay, the displacement is similar in the case of both axles which can be explained by the rigid suspension. The acceleration and the frequency of the body are shown in Figure 5.

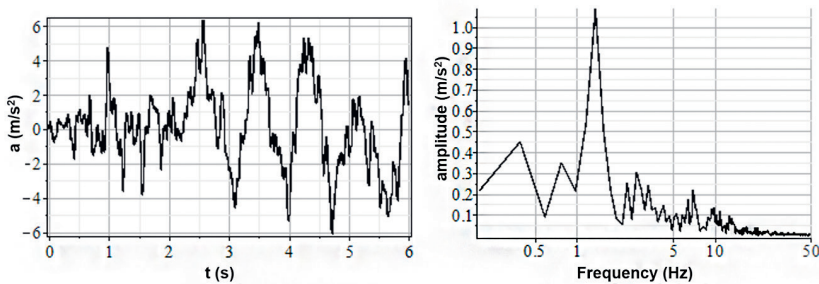


Figure 5: Acceleration of the body (left) and frequency diagram (right)  
 Source: Compiled by the authors.

The maximum acceleration of the body is  $6.359 \text{ m/s}^2$ . The peak frequency is  $1.37 \text{ Hz}$ , which corresponds to the scientific literature.<sup>29</sup>

This simulation was compared to measurement results.<sup>30</sup> The acceleration and the frequency diagram of the measurement is shown in Figure 6. It can be seen that the maximum of acceleration is larger than in the case of the simulation. This can be explained by the larger road irregularities for example potholes. Also the parameters were taken from the literature of a similar heavy-duty truck and were not measured exactly. In the field measurement there was a longer road segment (around  $500 \text{ m}$ ), while because of the long simulation time in the simulation it was  $100 \text{ m}$ . Therefore, not exactly the same road segment was measured during the field measurement. The accelerometer was also not placed exactly at the centre of gravity of the superstructure. It can be also seen that the peak frequency is  $1.88 \text{ Hz}$ , which is larger than in the simulation. The explanation can be that during the field measurement more points were recorded. A further research task is to improve the simulation model based on the field measurements.

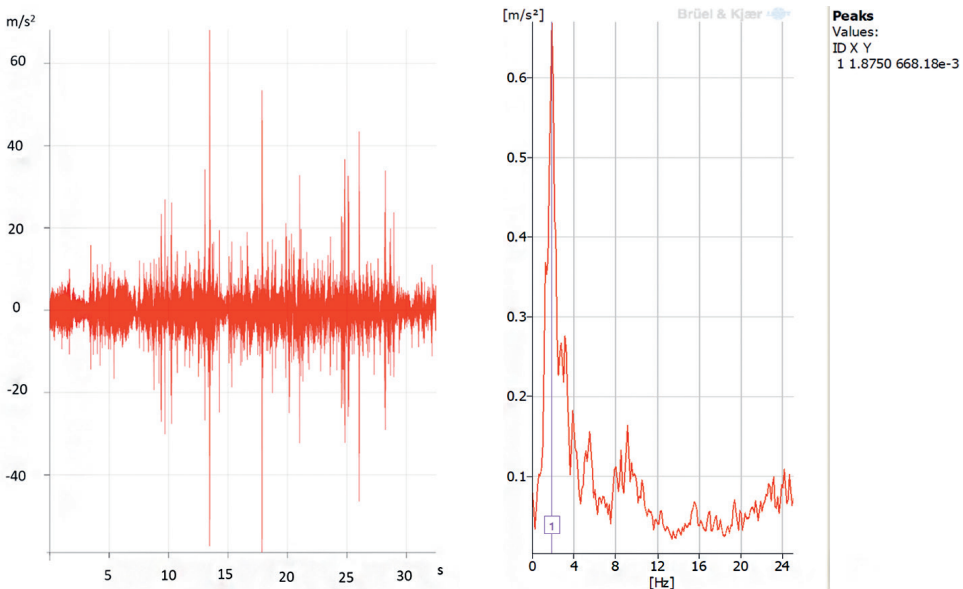


Figure 6: Measured acceleration (left) and frequency diagram (right)  
Source: Compile by the authors.

<sup>29</sup> GEBRESENBET et al. 2011: 10–19; HASSAN–MCMANUS 2002: 65–75.

<sup>30</sup> More details about the measurements can be found in HAJDU et al. 2019: 51–62.

## Conclusion

In this paper, the road profile modelling for a heavy-duty fire truck simulation was presented. To generate random road profiles a sinusoidal approach was selected based on road profile measurements. The road profiles were implemented as spline functions in the vehicle simulation. The fire truck was modelled as a full vehicle model to generate 2 different road profiles to the left and right sides. The peak frequency of the vehicle's acceleration is 1.4 Hz, which is similar to the results of other researches and corresponds to the value found in the available literature. The use of a full vehicle model allowed more accurate simulations, therefore a time delay between the front and rear axle was also observed. In the course of the analyses, a model was established taking into account the parameters of the heavy-duty firefighting vehicle. It provided a suitable starting point for obtaining accurate simulation results, therefore, in our opinion, it can be used for testing the suspension system of other vehicles with special superstructures, such as military vehicles. Further research tasks include a frequency-based analysis to obtain the harmful effects of road irregularities more precisely and use other road profile generation methods like white noise filtration. An important research task will be road profile generation based on field measurement and to improve the simulation model according to measurements. Other important tasks are to include the nonlinear effects of the vehicle and to obtain the fatigue damage.

## References

- AGOSTINACCHIO, Michele – CIAMPA, Donato – OLITA, Saverio (2014): The Vibrations Induced by Surface Irregularities in Road Pavements – A Matlab® Approach. *European Transport Research Review*, 6(3), 267–275. Online: <https://doi.org/10.1007/s12544-013-0127-8>
- BOGSJÖ, Klas – RYCHLIK, Igor (2009): Vehicle Fatigue Damage Caused by Road Irregularities. *Fatigue and Fracture of Engineering Materials & Structures*, 32(5), 391–402. Online: <https://doi.org/10.1111/j.1460-2695.2009.01340.x>
- BURDZIK, Rafal – KONIECZNY, Łukasz (2014): Vibration Issues in Passenger Car. *Transport Problems*, 9(3), 83–90.
- COST 354 (2007): *Performance Indicators for Road Pavement*. Work package WG2: Individual Performance Indicators. Report. Online: [http://cost354.zag.si/fileadmin/cost354/2wpr/COST354\\_WP2\\_Report\\_30052008.pdf](http://cost354.zag.si/fileadmin/cost354/2wpr/COST354_WP2_Report_30052008.pdf)
- DHARANKAR, Chandrashekhara S. – HADA, Mahesh K. – CHANDEL, Sunil (2017): Numerical Generation of Road Profile through Spectral Description for Simulation of Vehicle Suspension. *Journal of the Brazilian Society of Mechanical Sciences and Engineering*, 39(6), 1957–1967. Online: <https://doi.org/10.1007/s40430-016-0615-6>
- ESHKABILOV, Sulaymon – YUNUSOV, Abdvokhid (2018): Measuring and Assessing Road Profile by Employing Accelerometers and IRI Assessment. *American Journal of Traffic and Transportation Engineering*, 3(2), 24–40. Online: <https://doi.org/10.11648/j.ajtte.20180302.12>
- FAHAD, Mohammad – NAGY, Richard – FULEKI, Peter (2022): Creep Model to Determine Rut Development by Autonomous Truck Axles on Pavement. *Pollack Periodica: An International Journal for Engineering and Information Sciences*, 17(1), 66–71. Online: <https://doi.org/10.1556/606.2021.00328>
- GÁSPÁR, László – HORVÁT, Ferenc – LUBLÓY, László (2011): *Közlekedési létesítmények élettartama* [Lifetime of Transport Facilities]. Győr: Universitas-Győr Kft.

- GÁSPÁR, László – KÁROLY, Róbert (2007): Útpályaszerkezetek makroérdességi és csúszásellenállási teljesítményi mutatói [Macro-roughness and Skid Resistance Performance Indicators of Road Structures]. *Közlekedéstudományi Szemle*, 57(11), 442–449. Online: [http://real-j.mtak.hu/11018/12/Kozlekedestudomanyi\\_2007\\_12.pdf](http://real-j.mtak.hu/11018/12/Kozlekedestudomanyi_2007_12.pdf)
- GEBRESENBET, Girma – ARADOM, Samuel – BULITTA, Fufa S. – HJERPE, Eva (2011): Vibration Levels and Frequencies on Vehicle and Animals during Transport. *Biosystems Engineering*, 110(1), 10–19. Online: <https://doi.org/10.1016/j.biosystemseng.2011.05.007>
- GILLESPIE, T. D. – SAYERS, M. (1981): *Role of Road Roughness in Vehicle Ride*. Washington, D.C.: Transportation Research Board, 60<sup>th</sup> Annual Meeting. Online: <https://onlinepubs.trb.org/Onlinepubs/trr/1981/836/836-003.pdf>
- HAJDU, Flóra – SZALAI, Péter – MIKA, Péter – KUTI, Rajmund (2019): Parameter Identification of a Fire Truck Suspension for Vibration Analysis. *Pollack Periodica: An International Journal for Engineering and Information Sciences*, 14(3), 51–62. Online: <https://doi.org/10.1556/606.2019.14.3.6>
- HASSAN, Rayya – MCMANUS, Kerry (2002): Perception of Low Frequency Vibrations by Heavy Vehicle Drivers. *Journal of Low Frequency Noise, Vibration and Active Control*, 21(2), 65–75. Online: <https://doi.org/10.1260/026309202761019516>
- HORVÁTH, Péter (2006): *A mechatronika alapjai II* [Basics of Mechatronics II]. Győr: Széchenyi István University.
- ISO 8608:2016: Mechanical Vibration Road Surface Profiles – Reporting of Measured Data.
- JIAO, Leijia (2013): *Vehicle Model for Tyre-Ground Contact Force Evaluation*. Master thesis, KTH Royal Institute of Technology. Online: [www.diva-portal.org/smash/get/diva2:872185/FULLTEXT01.pdf](http://www.diva-portal.org/smash/get/diva2:872185/FULLTEXT01.pdf)
- KOVTUN, Vadim A. – KOROTKEVICH, Sergey G. – ZHARANOV, Vitaliy A. (2018): Computer Simulation and Research of the Stress-Strain State of Fire Tank Truck Construction. *Journal of Civil Protection*, 2(1). Online: <https://doi.org/10.33408/2519-237X.2018.2-1.81>
- KOVTUN, Vadim – KOROTKEVICH, Sergey G. – MIRCHEV, Yordan – LODNYA, Vyacheslav (2019): Optimization of Fire Truck's Tanks on the Chassis MAZ-6317 by the Method of Computer Simulation. *International Journal "NDT Days"*, 2(4), 495–500. Online: [www.ndt.net/article/NDTDays2019/papers/JNDTD-v2-n4-a16.pdf](http://www.ndt.net/article/NDTDays2019/papers/JNDTD-v2-n4-a16.pdf)
- LAKUŠIĆ, Stjepan – BRČIĆ, Davor – TKALČEVIĆ LAKUŠIĆ, Višnja (2011): Analysis of Vehicle Vibrations – New Approach to Rating Pavement Condition of Urban Roads. *Promet – Traffic & Transportation*, 23(6), 485–494. Online: <https://doi.org/10.7307/ptt.v23i6.183>
- LEE, Jeong-Hwan – LEE, Sang-Ho – KANG, Do-Kyung – NA, Sang-Do – YOO, Wan-Suk (2017): Development of a 3D Road Profile Measuring System for Unpaved Road Severity Analysis. *International Journal of Precision Engineering and Manufacturing*, 18(2), 155–162. Online: <https://doi.org/10.1007/s12541-017-0021-8>
- LENKUTIS, Tadas – ČERŠKUS, Aurimas – ŠEŠOK, Nikolaj – DZEDZICKIS, Andrius – BUČINSKAS, Vytautas (2021): Road Surface Profile Synthesis: Assessment of Suitability for Simulation. *Symmetry*, 13(1). Online: <https://doi.org/10.3390/sym13010068>
- LI, W. – SUN, Z. – HAO, Xuming – FENG, Xia-Ting (2015): Measuring Method for Asphalt Pavement Texture Depth Based on Structured-Light Technology. *Advances in Transportation Studies*, 36, 75–84. Online: [www.atsinternationaljournal.com/index.php/2015-issues/xxx-vi-july-2015/582-measuring-method-for-asphalt-pavement-texture-depth-based-on-structured-light-technology](http://www.atsinternationaljournal.com/index.php/2015-issues/xxx-vi-july-2015/582-measuring-method-for-asphalt-pavement-texture-depth-based-on-structured-light-technology)
- LITAK, Grzegorz – BOROWIEC, Marek – FRISWELL, Michael I. – SZABELSKI, Kazimierz (2008): Chaotic Vibration of a Quarter-Car Model Excited by the Road Surface Profile. *Communications in Nonlinear Science and Numerical Simulation*, 13(7), 1373–1383. Online: <https://doi.org/10.1016/j.cnsns.2007.01.003>
- MATSIKA, Emmanuel (2001): *Modelling of the Effect of Potholes on Motor Vehicle Structures*. Master thesis, University of Zambia. Online: <http://dspace.unza.zm/bitstream/handle/123456789/598/MatsikaE0001.PDF?sequence=1&isAllowed=y>

- MÚČKA, Peter (2018): Simulated Road Profiles According to ISO 8608 in Vibration Analysis. *Journal of Testing and Evaluation*, 46(1). Online: <https://doi.org/10.1520/JTE20160265>
- ŞENDUR, Polat – KURTDERE, Ali – AKALYAR, Oral (2013): A Methodology to Improve Steering Wheel Vibration of a Heavy Commercial Truck. *SAE Technical Paper*, 2013-01-2351. Online: [www.ingen-taconnect.com/contentone/ince/incep/2016/00000253/00000007/art00120?crawler=true](http://www.ingen-taconnect.com/contentone/ince/incep/2016/00000253/00000007/art00120?crawler=true)
- TYAN, Feng – HONG, Yu-Feng – TU, Shun-Hsu – JENG, Wes S. (2009): Generation of Random Road Profiles. *Journal of Advanced Engineering*, 4(2), 151–156.
- YOUSEFZADEH, Mahdi – AZADI, Shahram – SOLTANI, Abbas (2010): Road Profile Estimation Using Neural Network Algorithm. *Journal of Mechanical Science and Technology*, 24(3), 743–754. Online: <https://doi.org/10.1007/s12206-010-0113-1>
- ZEIDI, Seyed M. J. – HOSEINI, Pedram A. – RAHMANI, Ali (2017): Modeling a Three-axle Truck and Vibration Analysis under Sinusoidal Road Surface Excitation. *International Journal of Science and Engineering Applications*, 6(9), 285–295. Online: <https://doi.org/10.7753/IJSEA0609.1006>
- ZHAO, Boyu – NAGAYAMA, Tomonori – XUE, Kai (2019): Road Profile Estimation, and Its Numerical and Experimental Validation, by Smartphone Measurement of the Dynamic Responses of an Ordinary Vehicle. *Journal of Sound and Vibration*, 457, 92–117. Online: <https://doi.org/10.1016/j.jsv.2019.05.015>
- ZHAO, Leilei – ZHOU, Changcheng – YU, Yuewei – YANG, Fuxing (2016): A Method to Evaluate Stiffness and Damping Parameters of Cabin Suspension System for Heavy Truck. *Advances in Mechanical Engineering*, 8(7), 1–9. Online: <https://doi.org/10.1177/1687814016654429>